12350 J. Agric. Food Chem. 2010, 58, 12350–12356
DOI:10.1021/jf102152q

JOURNAL OF AGRICULTURAL AND FOOD CHEMISTRY
ARTICLE

Sorption of Deisopropylatrazine on Broiler Litter Biochars

Minori Uchimiya,* Lynda H. Wartelle, Isabel M. Lima, and K. Thomas Klasson

USDA-ARS Southern Regional Research Center, 1100 Robert E. Lee Boulevard, New Orleans, Louisiana 70124, United States

Biochars have received increasing attention in recent years because of a large-scale soil amendment to improve soil fertility, immobilize contaminants, and to serve as a recalcitrant carbon stock. Information is currently lacking in factors controlling the sorption capacity of manure-derived biochars. In this study, sorption isotherms for deisopropylatrazine, a stable metabolite of the widely applied herbicide atrazine, were obtained in acidic aqueous media (pH 5.5) for broiler litter-derived biochars formed by pyrolysis at 350 and 700 °C with and without steam activation at 800 °C. An increase in the Freundlich distribution coefficient (K_F) and isotherm nonlinearity (n_F) was observed with pyrolysis temperature and steam-activation, suggesting that the surface area and aromaticity (degree of carbonization) are the factors controlling the sorption capacity of chars at low surface coverage. At high surface coverage, the isotherms became increasingly linear, suggesting sorption on noncarbonized fraction of biochars. In binary-solute experiments, the sorption of deisopropylatrazine was significantly diminished by Cu^{II}, further suggesting the predominance of the surface adsorption mechanism at low surface coverage of biochars.

KEYWORDS: Biochar; deisopropylatrazine; copper; broiler litter; activated carbon

INTRODUCTION

Char is a form of environmental black carbon (BC), a ubiquitous carbonaceous geosorbent in soils and sediments (*1*). In recent years, BC has received a renewed interest as a large scale soil/sediment amendment for a wide range of environmental and agricultural applications including contaminant immobilization, soil fertilization, and carbon sequestration (*2*). Black carbon is composed of short stacks of polycyclic aromatic sheets "arranged in highly disordered fashion to form a poorly interconnected microporous network" and oxidized edge functional groups (*3*). Black carbon is particularly effective for the sorption of planar, hydrophobic, and aromatic compounds such as polycyclic aromatic hydrocarbons (PAHs) and planar polychlorinated biphenyls (PCBs) that are able to engage in face to face orientation with the graphene planes (*3*). Because the smallest pores are filled first, sorption is more favorable at low surface coverage (*4*). Consequently, nonlinear adsorption on BC in soils and sediments dominates at low equilibrium solute concentration (C_e) to solubility (S_w) ratios (*5*). A large number of studies have been conducted to elucidate the sorption mechanisms of both natural and synthetic BC for polar and nonpolar solutes (*5*). However, quantitative prediction of sorption capacity remains to be a challenge for biochars synthesized from different biomass sources, pyrolysis conditions, and pre- and post-treatments.

For activated carbons, linear solvation energy relationships (LSER) have been developed on the basis of sorbate activity, characteristic volume, polarity/polarizability, and basicity (*4*). The LSER suggested that for different activated carbons and sorbates, similar surface interactions dominate across the isotherm (C_e/S_w): (1) free energy gain from moving the sorbate from the solution to the hydrophobic surface (sorbate dispersion) and (2) replacement of hydrogen bonding in water by π-electrons of the extended aromatic surface (*4*). For example, LSER obtained from the Freundlich distribution coefficient (K_F) for 14 sorbates on Aldrich activated carbon (specific surface area = 556 $m^2\ g^{-1}$) showed a direct correlation with dispersion, an inverse correlation with the electron donating nature, and a weak correlation with the polarity of sorbate (*4*). For a class of compounds, sorbates with lower solubility and higher hydrophobicity showed greater tendency to sorb at any starting concentration (*4*).

Pyrolysis temperature impacts the degree of carbonization (development of surface area and aromaticity resulting from graphitization of the source material) (*6*) and the relative importance of adsorption (on carbonized fraction) and partitioning (on noncarbonized fraction) mechanisms (*7*). Plant-derived chars formed at incremental pyrolysis temperatures (e.g., 300−700 °C in 100 °C intervals (*7*)) suggested that polarity, aromaticity, surface area, and pore size distribution of char control the sorption capacity for both nonpolar and polar solutes (*7*,*8*). Studies employing natural organic matter (NOM) provided further evidence for determining the roles of sorbent surface area, polarity, and surface charge. The NOM reduced pesticide sorption on BC by blocking the micropore and increasing surface acidity (*9*, *10*). Inhibition by NOM was greater for larger molecules (from benzene and naphthalene to phenanthrene), and a concurrent increase in isotherm linearity was observed (*11*).

Deisopropylatrazine (**Table 1**) is found in groundwater and surface waters as a stable metabolite of the widely applied herbicide atrazine, and it is a suspected endocrine disruptor (*12*). The use of

*Corresponding author. Phone: (504) 286-4356. Fax: (504) 286-4367. E-mail: sophie.uchimiya@ars.usda.gov.

 Published on Web 11/04/2010

Table 1. Physical Properties of Deisopropylatrazine and Structurally Related Compounds[a]

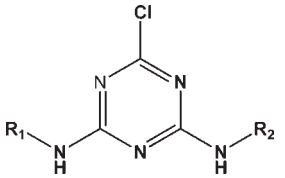

compound	R_1	R_2	log K_{ow}	pK_a	aqueous solubility (mg L^{-1})
deisopropylatrazine	CH_2CH_3	H	0.99	2.6 ± 0.5	670
atrazine	CH_2CH_3	$CH(CH_3)_2$	2.57	2.4 ± 0.5	33
simazine	CH_2CH_3	CH_2CH_3	2.12	3.1 ± 0.5	5
propazine	$CH(CH_3)_2$	$CH(CH_3)_2$	2.26	2.4 ± 0.5	3.8−8.6
deethylatrazine	H	$CH(CH_3)_2$	1.31	2.4 ± 0.4	3200
didealkylatrazine	H	H	0.35	2.6 ± 0.5	N/A

[a] Aqueous solubility and pK_a were obtained from ref *12*, and log K_{ow} was obtained from ref *34*.

activated carbons for the removal of triazine pesticides and metabolites (**Table 1**) such as deisopropylatrazine has been widely investigated (*12*). In addition, sawdust-derived biochar (*13*) and wheat ash (*9*) amendments in soil enhanced the retention of agrochemicals such as atrazine, acetochlor, and diuron. While atrazine has been employed in previous BC sorption studies as a model aromatic nonplanar bipolar compound having free electron pairs (*1*), sorptive interaction between chloro-*s*-triazines and carbonaceous materials is confounded by complex mechanisms. Despite similar physical properties (log K_{ow}, polarizability, planarity), atrazine sorbed on BC-rich (combusted) sediment to a lesser extent than diuron (*1*). On carbon nanotubes, hydrogen bonding interaction was observed between surface functional groups and azo and amino nitrogen of atrazine (*14*). Atrazine, having a melting point of 174 °C (*15*), may condense as a solid when adsorbed on carbonaceous materials (*16*). Crystalline phases in adsorbed state cannot pack as tightly as the liquid state, and are less effective in filling pores (*16*). In addition, inhibition by the native organic phases of chars is greater for compounds that adsorb as solid (*16*).

In comparison to plant-derived chars, little information is available for predicting the sorption capacity of manure-derived chars. Manure-derived biochars are expected to be a particularly useful soil fertilizer, as well as soil conditioner, because of high leachable nutrient contents (*17*). In order to predict the fate of agrochemicals and their metabolites in soils amended with manure-derived biochar, fundamental knowledge is necessary on the factors controlling the sorption capacity of manure chars. In this study, broiler litter-derived chars formed by pyrolysis at 350 and 700 °C and steam-activated analogues were investigated for the sorption of deisopropylatrazine in acidic aqueous media. Sorption isotherms were compared to the specific surface area, aromaticity, and polarity of biochars. Considering the ability of manure-derived chars to (1) sorb metal ions and (2) release forms of nutrients (e.g., P, N, and S) that may complex metal ions, the effect of selected metal ions (Cu^{II}) on the sorption of deisopropylatrazine was also investigated. Of heavy metal contaminants, copper was selected because of its occurrences in high concentration in arms range soils (*18*) and particular sensitivity to complexation by soluble ligands (*19*).

MATERIALS AND METHODS

Chemicals. All chemical reagents were of the highest purity available and were used as received. Copper(II) nitrate trihydrate was obtained from Acros Organics (Morris Plains, NJ). Anhydrous sodium acetate, glacial acetic acid, and ethyl acetate were obtained from J. T. Baker (Phillipsburg, NJ). Analytical standard grade (PESTANAL; 95.4% HPLC assay) deisopropylatrazine was obtained from Sigma-Aldrich (Milwaukee, WI), and 250 ppm stock solution was prepared daily in 0.1 M acetate buffer (pH 5.5). Distilled, deionized water (DDW) with a resistivity of 18 MΩ cm (Millipore, Milford, MA) was used for all procedures. **Table 1** provides the physical properties of deisopropylatrazine. All sorption experiments were performed in 0.1 M acetate buffer (pH 5.5) to (1) maintain the neutral form of deisopropylatrazine (pK_a = 2.6, **Table 1**) and (2) minimize the precipitation of copper.

Biochar Preparation and Characterization. As described in a previous report (*20*), broiler litter samples were obtained from USDA-ARS Poultry Research Unit (Starkville, MS), milled to less than 1 mm (< 25% moisture content), and pelletized to cylinders of approximately 5 mm diameter and 5 mm length, and pyrolyzed at either 350 or 700 °C for 1 h under 0.1 $m^3 h^{-1}$ nitrogen flow rate. The resulting chars (350BL and 700BL) were allowed to cool to room temperature overnight in the retort. Activated analogues of 350BL and 700BL (350ABL and 700ABL, respectively) were prepared by steam activation (3 mL min^{-1} water flow rate) at 800 °C for 45 min under nitrogen, following the pyrolysis step. Pyrolyzed samples were washed with 0.1 M HCl (27 g char L^{-1}) by constant stirring for 1 h, rinsed three times with DDW, dried overnight at 80 °C, and then ground and sieved to less than 44 μm (325 mesh).

Surface areas were measured in duplicate by nitrogen adsorption isotherms at 77 K using a NOVA 2000 surface area analyzer (Quantachrome, Boynton Beach, FL). Specific surface areas were determined from adsorption isotherms using the Brunauer, Emmett, and Teller (BET) equation. Elemental composition (CHNSO) was determined by dry combustion using a Perkin-Elmer 2400 Series II CHNS/O analyzer (Perkin-Elmer, Shelton, CT). Surface functional groups of all biochars employed in this study were rigorously characterized in a previous report by ATR-FTIR, ^{1}H NMR, and Boehm titration (*21*).

Sorption Kinetics. Separate suspensions of 350BL and 350ABL in 15 mL of 0.1 M acetate buffer (pH 5.5) were preequilibrated for 24 h by shaking end-overend at 70 rpm in amber glass vials. End-over-end rotation (70 rpm) was employed for all subsequent procedures. Reaction was initiated by adding 15 mL of 250 ppm deisopropylatrazine stock solution in acetate buffer to achieve the initial deisopropylatrazine concentration of 125 ppm. Char loadings were set to 3.3 g L^{-1} for 350BL and 1.7 g L^{-1} for 350ABL. At successive time intervals (4, 8, 24, 72, and 96 h), suspensions were removed from the end-over-end shaker and filtered (0.2 μm Millipore Millex-GS). The filtrate (20 mL) was extracted with 5 mL of ethyl acetate by shaking for 30 min after the addition of 20 μL of internal standard (Restek 527 internal standard mix, Sigma-Aldrich). Deisopropylatrazine concentration in ethyl acetate extract was determined using GC-MS (Agilent 6890N GC equipped with a 5890N MS detector; Agilent Technologies, Santa Clara, CA) in scan mode with the transfer line temperature of 180 °C. Splitless mode was employed using a capillary column (30 m × 0.25 mm Restek Rxi-5 ms; Restek U.S., Bellefonte, PA) with the injector temperature of 180 °C. The 173 *m*/*z* ion peak was monitored for deisopropylatrazine, and the 188 *m*/*z* ion peak was monitored for the d_{10} phenanthrene internal standard.

Sorption Isotherms. All sorption isotherms were obtained in duplicate, and the total volume of each reactor was set to 30 mL. Sorption isotherms

Table 2. Surface Areas[a] and Elemental Compositions[b] of Chars Employed in This Study[c]

char	BET surface area ($m^2\ g^{-1}$)	micropore area ($m^2\ g^{-1}$)	micropore volume ($mL\ g^{-1}$)
700ABL	335 ± 1	278 ± 4	0.136 ± 0.002
350ABL	335 ± 7	277 ± 5	0.134 ± 0.001
700BL	94 ± 5	42 ± 2	0.018 ± 0.001
350BL	60 ± 20	0	0

char	C % (w/w)	H % (w/w)	N % (w/w)	S % (w/w)	O % (w/w)	H/C	O/C	(O+N)/C	(O+N+S)/C
350BL	45.6 ± 0.5	4.0 ± 0.1	4.5 ± 0.1	0.7 ± 0.1	18.3 ± 0.2	1.06 ± 0.01	0.301 ± 0.001	0.385 ± 0.001	0.391 ± 0.001
700BL	46.0 ± 0.1	1.42 ± 0.03	2.82 ± 0.02	1.0 ± 0.1	7.4 ± 0.9	0.37 ± 0.01	0.12 ± 0.02	0.17 ± 0.02	0.18 ± 0.02
350ABL	30 ± 1	1.14 ± 0.03	1.85 ± 0.09	0.6 ± 0.1	10.5 ± 0.8	0.45 ± 0.03	0.26 ± 0.01	0.31 ± 0.01	0.32 ± 0.01
700ABL	29 ± 1	1.14 ± 0.04	1.72 ± 0.04	0.8 ± 0.1	10.7 ± 0.1	0.47 ± 0.01	0.28 ± 0.02	0.33 ± 0.02	0.34 ± 0.02
manure	34.8 ± 0.4	5.4 ± 0.1	6 ± 2	1.3 ± 0.1	31.0 ± 0.8	1.85 ± 0.01	0.67 ± 0.01	0.81 ± 0.06	0.82 ± 0.05

[a] BET results were obtained from ref *21*. [b] Elemental compositions were not corrected for ash or moisture contents. Except for manure, CHNS values were obtained from ref *35*. H/C, O/C, (O + N)/C, and (O + N + S)/C are give as molar ratios. [c] Values are given as the mean ± standard deviation for duplicate (surface areas) or triplicate (elemental composition) measurements.

for 350BL, 700BL, 350ABL, and 700ABL were obtained after 72 h of equilibration by following the methods described above for kinetic experiments. Biochar loadings were set to 3.3 g L^{-1} for 350BL and 700BL and 1.7 g L^{-1} for 350ABL and 700ABL. Initial deisopropylatrazine concentration was set to 0−200 ppm by adjusting the volume of 250 ppm stock solution.

Copper sorption isotherms were obtained for 350BL (3.3 g L^{-1}) and 350ABL (1.7 g L^{-1}). Initial Cu^{II} concentrations were set to 0−800 ppm by adjusting the volume of 1000 ppm stock solution in 0.1 M acetate buffer (pH 5.5). For 350BL, equilibrium concentrations of additional elements (P, K, S, Ca, Na, and Al) were determined for selected isotherm points. The same procedure was followed as described above for deisopropylatrazine, except for the following modifications. Instead of ethyl acetate extraction, the filtrate was acidified to 4% (v/v) nitric acid (trace metal grade, Sigma-Aldrich) for the determination of Cu, P, K, S, Ca, Na, and Al concentrations using an inductively coupled plasma optical emissions spectrometer (ICP-AES; Profile Plus, Teledyne/Leeman Laboratories, Hudson, NH).

In order to test for the competitive sorption of deisopropylatrazine and Cu^{II}, additional sorption experiments were conducted for (1) 50 ppm deisopropylatrazine + 50 ppm Cu^{II}, (2) 100 ppm deisopropylatrazine + 100 ppm Cu^{II}, and (3) 200 ppm deisopropylatrazine + 200 ppm Cu^{II} for 350BL (3.3 g L^{-1}) and 350ABL (1.7 g L^{-1}). Both Cu^{II} and deisopropylatrazine concentrations were determined for each isotherm point.

RESULTS AND DISCUSSION

Biochar Characterization. Table 2 provides BET surface area, micropore area, and volume, and CHNSO content (in weight percent; values were not corrected for ash and moisture contents) of chars. Surface areas increased with pyrolysis temperature and by activation, in the following order: 350BL < 700BL ≪ 350ABL ≈ 700ABL. The H, N, and O contents showed a decreasing trend with pyrolysis temperature and activation: manure > 350BL > 700BL > 350ABL ≈ 700ABL (H and N); manure > 350BL > 350ABL ≈ 700ABL > 700BL (O). In contrast, C content increased by pyrolysis (350BL and 700BL) and decreased by steam-activation (350ABL and 700ABL), relative to the source material (manure). The S content was the lowest and was approximately 1% for all biochars.

Molar ratios of elements were determined to estimate the aromaticity (H/C ratio) and polarity (O/C, (O + N)/C, and (O + N + S)/C ratios) of chars (*8*) (**Table 2**). All molar ratios in **Table 2** show a decreasing trend with pyrolysis temperature and steam activation: manure > 350BL > 350ABL ≈ 700ABL > 700BL. Hence, aromaticity increased and polarity decreased with pyrolysis temperature and steam activation, and the highest aromaticity and lowest polarity was observed for 700BL. A previous study on wheat residue (*7*) and pine needle chars (*8*) showed a sequential (1) decrease in the molar ratios of O/C and H/C as well as the H and O contents, and (2) increase in C content with pyrolysis temperature (100−700 °C in 100 °C increment). The observed trend was attributed to (1) the removal of polar surface functional groups and (2) the formation of aromatic structures by a higher degree of carbonization of the organic source material (*7*, *8*). In contrast, dairy manure-derived chars showed an increase in the O content and the O/C ratio, and a decrease in the C, H, and N contents and the H/C ratio with an increase in pyrolysis temperature from 25 (unpyrolyzed dairy manure), 200, to 350 °C (*22*). Therefore, while an increase in aromaticity (decrease in H/C ratio) was consistently observed, the impact of pyrolysis temperature and activation on polarity greatly differ for manure- and plant-derived chars. Contrasting effects of pyrolysis temperature on surface functional groups (that contribute to the polarity of chars) of plant- and manure-based chars were also observed in Boehm titration and FTIR results (*21*). Previous elemental analyses reported 5.9% (w/w) nitrogen and 0.8% (w/w) sulfur contents of broiler manure (*23*). Broiler litter char contained 3.7% (w/w) phosphorus and 1.7% (w/w) sulfur (*20*). The viscous portion of biooil derived by fast pyrolysis of broiler manure at 350 °C contained 6.3% (w/w) nitrogen, 0.5% (w/w) sulfur, and 0.04% (w/w) phosphorus (*23*).

Sorption of Deisopropylatrazine. Deisopropylatrazine sorption isotherms were obtained at pH 5.5 (0.1 M acetate buffer) after 3 days of equilibration. All sorption experiments were performed at <30% aqueous solubility (**Table 1**) of deisopropylatrazine. Kinetic experiments indicated that equilibrium was reached within the equilibration period employed (Figure S1, Supporting Information). Similar sorption kinetics (2−3 days to reach apparent equilibrium) was observed for atrazine on dairy manure chars (*22*) and naphthalene and nitrobenzene on wood and crop residue chars (*8*). In a study employing Aldrich activated carbon (556 $m^2\ g^{-1}$ surface area), toluene sorption reached equilibrium after 3 days (*4*). For the larger molecule pyrene, equilibrium was not reached for more than a month (*4*). Diffusive penetration into the porous surface was postulated to be the factor controlling the sorption kinetics (*4*).

Figure 1 provides the concentration of deisopropylatrazine sorbed on chars on a dry weight basis (q_e in mg g^{-1}) as a function of deisopropylatrazine concentration remaining in solution (C_e in mg L^{-1}) at equilibrium for low C_e/S_w (≤0.02). Sorption isotherms were fit to the Freundlich equation (lines in **Figure 1**) to allow for comparison with previous reports on contaminant sorption by carbonaceous materials:

$$\log q_e = n_F \log C_e + \log K_F \quad (1)$$

where K_F is the Freundlich distribution coefficient, and n_F is the Freundlich exponent. The n_F coefficient typically ranges from

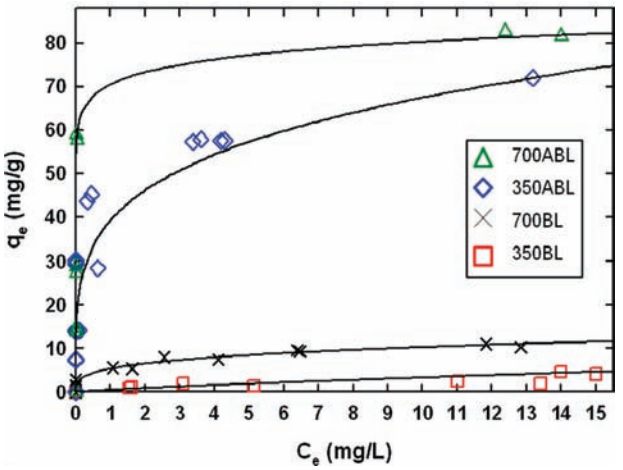

Figure 1. Deisopropylatrazine sorption isotherms for 350BL, 700BL, 350ABL, and 700ABL. Lines represent the model fit to the Freundlich isotherm (**Table 3**).

Table 3. Freundlich Parameters for the Sorption of Deisopropylatrazine

char	log K_F (L kg^{-1})	n_F	R^2
350BL	3.27	0.81	0.88
700BL	5.89	0.29	0.90
350ABL	6.89	0.23	0.81
700ABL	7.68	0.06	0.94

0.24 to 1.0 for BC and is below 1 for nonlinear isotherms (*24*). Nonlinearity arises from variable site geometries and energetic and saturation of surface adsorption sites (*24*), especially micropores with pore diameters below 2 nm (*25*).

Table 3 provides K_F (in L kg^{-1}) and n_F parameters obtained for broiler litter chars. An increasing trend in K_F, indicative of the higher sorption capacity of char, was observed with higher pyrolysis temperature and activation: 350BL < 700BL < 350ABL < 700ABL. Correspondingly, a decrease in n_F, indicative of the increasing nonlinearity of isotherms, was observed: 350BL > 700BL > 350ABL > 700ABL. The trends in **Table 3** indicate that both the sorption capacity (K_F) and nonlinearity of the isotherm (n_F) are enhanced by higher pyrolysis temperature and by activation. The nonlinearity at low equilibrium concentration (0−15 ppm C_e, **Figure 1**) to solubility (S_w of 670 ppm, **Table 1**) ratio employed in **Figure 1** ($C_e/S_w \leq 0.02$) results from the saturation of surface adsorption sites (*8*). The higher n_F value for 350BL formed at lower temperature (**Table 3**) indicates an increasingly nonlinear nature of the isotherm for chars having higher BET surface area (**Table 2**).

A previous study on dairy manure chars formed at low pyrolysis temperatures reported a linear atrazine sorption isotherm within the range where a commercial activated carbon showed saturation (*22*). Linear isotherms of chars, having low specific surface areas (2.62 m^2 g^{-1} for char formed at 200 °C and 6.84 m^2 g^{-1} for 350 °C) (*22*), were attributed to the predominance of the partitioning mechanism (on organic fraction) over surface adsorption (on carbonized fraction). Transition from linear to nonlinear isotherms with pyrolysis temperature has been observed for both polar and nonpolar aromatic compounds such as naphthalene, nitrobenzene (*8*), and benzene (*26*) in studies employing plant-derived chars.

Figure 2a,**b** shows a linear increase in log K_F and a decrease in n_F as a function of log (BET surface area) of biochars. While the molar H/C ratios for 700BL, 350ABL, and 700ABL are close to one another, the lowest log K_F and highest n_F of 350BL correlate

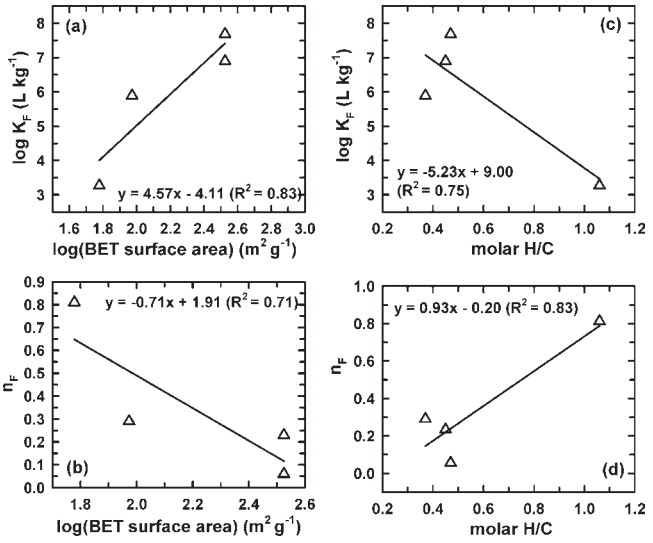

Figure 2. Freundlich distribution coefficient (log K_F) and exponent (n_F) versus log (BET surface area) (**a**,**b**) and molar H/C ratio (**c**,**d**). Lines represent linear regression. Values were obtained from **Tables 2** and **3**. Correlation slightly decreased when absolute values were used for the BET surface area: (**a**) $y = 0.011x + 3.65$ ($R^2 = 0.74$); (**b**) $y = 0.0017x + 0.70$ ($R^2 = 0.61$).

with the highest H/C ratio (**Figure 2c**,**d**). While linear correlation was not observed between log K_F and the polarity of chars (O/C, (O + N)/C, and (O + N + S)/C ratios), log K_F was higher for chars with lower polarity (**Tables 2** and **3**).

A previous study on propanil reported a similar dependence of K_F on surface areas of rice straw-derived chars (*10*). The dependence on surface area indicates the importance of pore-filling mechanism (*16*). For aromatic sorbates, the specific interaction with aromatic π-systems of BC provides additional sorptive forces (*27*). Polycondensed aromatic structures of BC result in delocalizing resonance effects throughout the fused π-system, making BC a strong π-donor (*27*). N-Heteroaromatic systems of deisopropylatrazine can function both as a π-donor and an acceptor (*27*). The importance of aromaticity (that leads to π-electron interactions) was evidenced by a linear decrease in log K_F and increase in n_F as a function of the molar H/C ratio of wheat residue-derived chars in the sorption of naphthalene and nitrobenzene (*8*).

Nonlinear Isotherms. Previous studies demonstrated a transition from the nonlinear to linear isotherm with increasing C_e/S_w for both polar and nonpolar solutes on plant-derived chars (*8*) and in soils (*28*). To test for the influence of C_e/S_w on the linearity of isotherms, sorption studies for 350BL and 700BL (**Figure 1**) were conducted at higher C_e/S_w (0.02−0.15; **Figure 3**). In **Figure 3**, biochar loading was set to 3.3 g L^{-1} for the entire C_e/S_w range employed for 350BL. For 700BL, 0.3 g L^{-1} was employed at high C_e/S_w (additional points in **Figure 3**) to achieve C_e above the detection limit at the initial concentration below S_w. At C_e/S_w between 0.02 (where saturation was observed in **Figure 1**) and 0.15, linear isotherms were obtained for both 350BL and 700BL (**Figure 3**). Similar to the lower C_e/S_w case (**Figure 1**), sorption on 700BL was significantly greater than on 350BL (**Figure 3**).

Transition from the nonlinear to linear isotherm for both 350BL and 700BL suggests complex sorptive interactions on heterogeneous sorbents (unaltered and pyrolyzed precursor material and ash) across C_e/S_w. The duration of pyrolysis (1 h in this study, versus 3−6 h in previous reports on plant (*8*) and manure (*22*) chars) can impact the relative proportion of carbonized (high surface area and aromaticity portion) and noncarbonized (remaining or

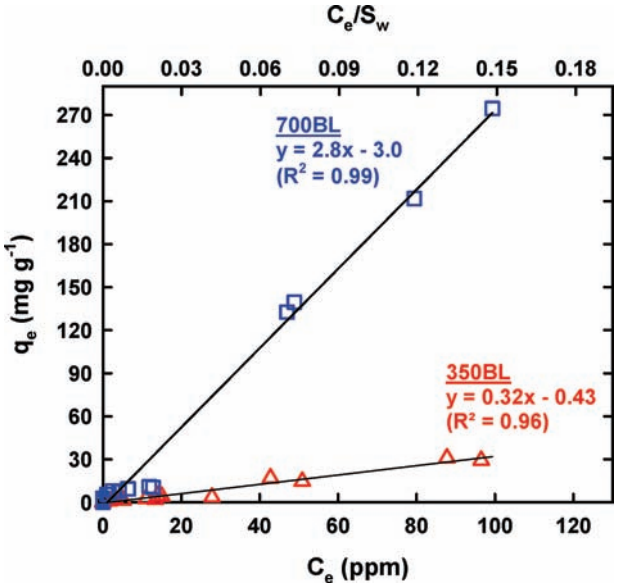

Figure 3. Transition from the nonlinear to the linear isotherm (C_e/S_w > 0.02) for the sorption of deisopropylatrazine on 350BL and 700BL. The *x*-axis is given in both C_e (bottom) and C_e/S_w (top). Lines represent the linear regression for 350BL (△) and 700BL (□).

partially altered source material) fractions. Transition from the nonlinear to linear isotherm has been attributed to the predominance of (1) adsorption on carbonized fractions at low C_e/S_w and (2) partitioning into noncarbonized fractions at high C_e/S_w (*8*).

Competition with Cu^{II}. Diamonds in **Figures 4b,c** show the concentration of Cu^{II} sorbed on 350ABL and 350BL on a dry weight basis (q_e in mg g^{-1}) versus equilibrium Cu^{II} concentration remaining in solution (C_e in mg L^{-1}). Copper sorption on 350BL (**Figure 4c**) was much lower than on 350ABL (**Figure 4b**), and the isotherm was more linear in nature. Both 350BL and 350ABL sorbed more deisopropylatrazine (**Figure 1**) than Cu^{II} (diamonds in **Figure 4b,c**) at respective C_e in single-solute experiments.

In order to determine the influence of leachable biochar fractions on Cu^{II} sorption, soluble concentrations of Na, Ca, P, K, and S were determined at selected initial Cu^{II} concentrations across the isotherm (0−780 ppm initial Cu^{II} concentrations) for 350BL in **Figure 4c** (diamonds). The highest Na concentration arises from sodium acetate used to buffer pH in all experiments (Figure S2, Supporting Information). While equilibrium Na, S, and P concentrations stayed within the error range (apart from the lower P for the highest initial Cu^{II} concentration, Figure S2, Supporting Information) across the isotherm (diamonds in **Figure 4c**), Ca and K showed a slight decreasing trend as a function of initial Cu^{II} concentration. However, equilibrium Ca and K concentrations were lower when copper was not added (Figure S2, Supporting Information). The results suggest cation exchange and additional complex mechanisms for copper sorption in the acidic aqueous system employed. For the sorption of Pb^{II} on dairy manure char produced at 350 °C, soluble P concentration remained low (< 100 μM), while Ca and Mg concentrations increased at sufficiently high initial Pb^{II} concentration (*22*). Low P concentration was attributed to the precipitation of Pb phosphate phases, while an increase in Ca and Mg was attributed to mineral dissolution (*22*).

Triangles in **Figure 4b,c** show Cu^{II} sorption isotherms for binary-solute experiments in which equal concentrations (50, 100, and 200 ppm) of Cu^{II} and deisopropylatrazine were added together to each reactor containing 350ABL or 350BL. In the presence of deisopropylatrazine, Cu^{II} sorption slightly diminished for 350ABL and slightly increased for 350BL. Triangles in

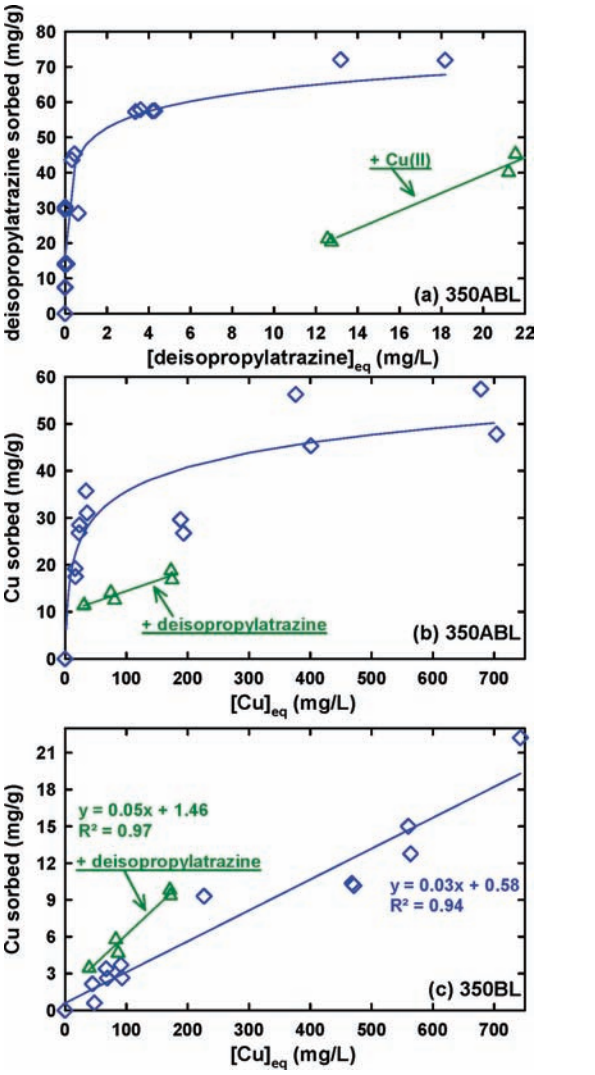

Figure 4. Sorption isotherms for deisopropylatrazine (**a**) and copper (**b**,**c**) on 350ABL (**a**,**b**) and 350BL (**c**) in single-solute (◇) and binary-solute (△) experiments. In **a**−**b**, the lines are drawn for visual aid and do not represent the model fit. In **c**, the lines represent linear regression.

Figure 4a show the deisopropylatrazine sorption isotherm on 350ABL for the same binary-solute experiment as in **Figure 4b**. The presence of Cu^{II} significantly diminished the sorption of deisopropylatrazine on 350ABL (**Figure 4a**).

Inhibition of deisopropylatrazine sorption on 350ABL by Cu^{II} at low C_e/S_w (**Figure 4a**) suggests that surface adsorption dominates for both deisopropylatrazine and Cu^{II} under the experimental conditions employed. The solution pH strongly impacts the sorption of metal cations on chars by controlling the speciation of both metal ions and the surface functional groups of char (*29*). Above pH_{pzc}, (1) attractive electrostatic interactions between the negatively charged biochar surface and metal cations and (2) metal ion complexation by surface functional groups (e.g., carboxylic, hydroxylic, and phenolic) become important (*30*). The sorptive interaction between metal ions and carbonaceous materials can inhibit the sorption of organic compounds in binary-solute systems. Copper and lead inhibited the sorption of both polar and nonpolar compounds such as atrazine, 1,2-dichlorobenzene, 2,4-dichlorophenol, and naphthalene on wood char (*14*), wheat ash (*31*), and carbon nanotubes (*14*). The complexation of metal ions by surface functional groups results in the formation of a dense hydration shell at surfaces that prevents

the access of organic compounds to surface adsorption sites (i.e., competition for available adsorption sites) (*22*, *31*). In contrast, softer Lewis acids such as Cd^{II} (*31*) and Ag^{I} (*14*), having lower affinity for oxygen-donor ligands, either increased or had no effects on the sorption of organic solutes.

In addition to sorption, there is a potential for the reduction of Cu^{II} by surface functional groups of biochars. Reduction of Cr^{VI} to Cr^{III} on rice straw-derived BC has been observed (*29*). The phenolic group on the BC surface is the putative reductant and becomes oxidized to carbonyl/carboxyl as a result of electron transfer events (*29*). In addition, the reduction of Cu^{II} by a nitrogen-containing agrochemical (daminozide) has been observed (*32*). Acid−base speciation and solubility of Cu greatly depends on its oxidation state. Copper(II) exists predominantly in Cu^{II}-hydroxo species until pH is raised to near-neutral for Cu^{II} (hydr)oxide formation (*32*). Copper(I), in contrast, is strongly complexed by halide ions (Cl^- and Br^-), and precipitation of Cu_2O(s) does not occur until the strongly alkaline pH range (*32*).

In conclusion, sorption capacity (K_F) and nonlinearity (n_F) of deisopropylatrazine sorption isotherms positively correlated with the BET surface area and aromaticity (H/C ratio) of broiler litter-derived biochars at low surface coverage ($C_e/S_w \leq 0.02$). In addition, the sorption of deisopropylatrazine was more favorable on chars with lower polarity (O/C, (O + N)/C, and (O + N + S)/C ratios). Hence, the higher degree of carbonization with increasing pyrolysis temperature (from 350 to 700 °C) and steam activation enhanced the sorption of deisopropylatrazine. At low surface coverage, surface adsorption on the carbonized fraction of biochars likely dominated. At higher surface coverage (C_e/S_w up to 0.15), a transition from the nonlinear to linear sorption isotherm was observed. In binary-solute experiments, Cu^{II} significantly diminished the sorption of deisopropylatrazine on 350ABL, even though sorption capacity (of both 350ABL and 350BL) was greater for deisopropylatrazine than Cu^{II} in single-solute experiments.

Additional Controlling Factors. In addition to the surface area and aromaticity of chars, the hydrophobicity of the solute controls the sorptive interactions with both chars and activated carbons. Octanol−water partition coefficient (log K_{ow}) is widely used as a measure of the hydrophobicity of organic contaminants. A previous study in sorption of a mixture of chloro-*s*-triazines by commercial activated carbons showed higher K_F for more hydrophobic (higher log K_{ow}) compounds in DDW at pH 7 (*12*) (Table S1, Supporting Information). Deisopropylatrazine sorbed to a lesser extent than more hydrophobic compounds such as atrazine, simazine, and propazine (Table S1, Supporting Information) (*12*). A plot of log K_F versus log K_{ow} shows a positive correlation for two different commercial activated carbons (Figure S3, Supporting Information). When experiments were conducted using river water, K_F values were significantly diminished for all solutes (*12*), and a linear correlation between log K_F and log K_{ow} was no longer observed. The results highlight the importance of NOM on the sorptive properties of carbonaceous materials in aqueous environments. A comparison of K_F values suggests that 700BL, 350ABL, and 700ABL exhibit analogues or greater sorption capacity for deisopropylatrazine, relative to the two commercial activated carbons, Calgon WPH and Norit HDB (Figure S3, Supporting Information). It must be noted that K_F values from the two studies were obtained under different (single and multiple solute) experimental conditions.

Equilibrium partition theory (EPT) (*24*), based on log K_{ow}, is often used to predict the sorption of persistent organic pollutants on NOM:

$$\log K_{oc} = 0.97 \log K_{ow} - 0.12 \quad (2)$$

where K_{oc} is the partitioning coefficient to organic carbon. Sorption on NOM is characterized by a fast, linear, and noncompetitive partitioning mechanism (*24*). Black carbon is responsible for the several orders of magnitude greater sorption capacity (than is predictable from EPT) of soils and sediments for planar and hydrophobic contaminants (*24*). The importance of NOM and BC as the sorptive capacity of soils and sediments has been reviewed (*5*, *24*) and is often described as "dual-mode sorption".

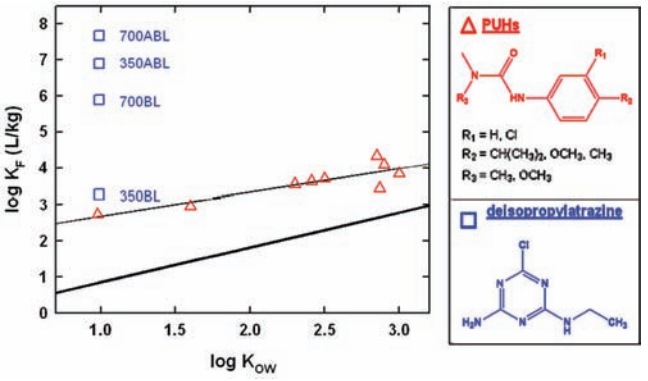

Figure 5. Impact of solute hydrophobicity (log K_{ow}) on the Freundlich distribution coefficient (log K_F) of deisopropylatrazine on broiler litter chars (blue squares, this study) and PUHs on NIST diesel soot (red triangles, ref *33*). The thin line represents the linear regression for PUHs: $y = 0.65x + 2.04$ ($R^2 = 0.76$). The thick line represents the prediction based on EPT (eq 2).

Figure 5 illustrates the sorptive forces of chars in addition to hydrophobic interactions. The thick line in **Figure 5** represents log K_{oc} calculated on the basis of EPT (eq 2). Triangles in **Figure 5** represent K_F for the sorption of phenyl urea herbicides (PUHs) on NIST diesel soot (*33*). The observed trend in **Figure 5** (higher K_F on BC than is predictable from EPT) for PUHs ($1 < \log K_{ow} < 3$) extends to more planar and hydrophobic organic pollutants such as PAHs and PCBs ($3 < \log K_{ow} < 8$) (*33*). The K_F values for deisopropylatrazine obtained from this study are shown as squares in **Figure 5**. While the K_F value for 350BL is close to the values predicted for NIST diesel soot (linear regression shown as a thin line in **Figure 5**), the values are significantly higher for 700BL, 350ABL, and 700ABL. Broiler litter biochar formed at high pyrolysis temperature (700BL) and steam-activated biochars (350ABL and 700ABL) showed 5−7 orders of magnitude greater K_F for deisopropylatrazine than is predictable from EPT. Depending on the formation conditions and precursor material, BC can possess a spectrum of surface area, ash, and volatile matter composition (*6*) that will impact in situ sediment/soil to water partition coefficients (*24*). Whether the purpose of biochar amendment is soil fertilization or carbon sequestration, the influence of biochars on the sorption behavior of amended soils must be considered.

Supporting Information Available: Deisopropylatrazine sorption kinetics, equilibrium soluble Na, Ca, P, K, and S concentrations for Cu^{II} sorption on 350BL, and sorption of deisopropylatrazine on commercial activated carbons. This material is available free of charge via the Internet at http://pubs.acs.org.

LITERATURE CITED

(1) Cornelissen, G.; Haftka, J.; Parsons, J.; Gustafsson, O. Sorption to black carbon of organic compounds with varying polarity and planarity. *Environ. Sci. Technol.* **2005**, *39*, 3688−3694.

(2) Roberts, K. G.; Gloy, B. A.; Joseph, S.; Scott, N. R.; Lehmann, J. Life cycle assessment of biochar systems: Estimating the energetic, economic, and climate change potential. *Environ. Sci. Technol.* **2010**, *44*, 827−833.

(3) Zhu, D. Q.; Kwon, S.; Pignatello, J. J. Adsorption of single-ring organic compounds to wood charcoals prepared under different thermochemical conditions. *Environ. Sci. Technol.* **2005**, *39*, 3990−3998.
(4) Shih, Y. H.; Gschwend, P. M. Evaluating activated carbon-water sorption coefficients of organic compounds using a linear solvation energy relationship approach and sorbate chemical activities. *Environ. Sci. Technol.* **2009**, *43*, 851−857.
(5) Cornelissen, G.; Gustafsson, O.; Bucheli, T. D.; Jonker, M. T. O.; Koelmans, A. A.; Van Noort, P. C. M. Extensive sorption of organic compounds to black carbon, coal, and kerogen in sediments and soils: Mechanisms and consequences for distribution, bioaccumulation, and biodegradation. *Environ. Sci. Technol.* **2005**, *39*, 6881−6895.
(6) Keiluweit, M.; Nico, P. S.; Johnson, M. G.; Kleber, M. Dynamic molecular structure of plant biomass-derived black carbon (biochar). *Environ. Sci. Technol.* **2010**, *44*, 1247−1253.
(7) Chun, Y.; Sheng, G. Y.; Chiou, C. T.; Xing, B. S. Compositions and sorptive properties of crop residue-derived chars. *Environ. Sci. Technol.* **2004**, *38*, 4649−4655.
(8) Chen, B. L.; Zhou, D. D.; Zhu, L. Z. Transitional adsorption and partition of nonpolar and polar aromatic contaminants by biochars of pine needles with different pyrolytic temperatures. *Environ. Sci. Technol.* **2008**, *42*, 5137−5143.
(9) Yang, Y. N.; Sheng, G. Y. Pesticide adsorptivity of aged particulate matter arising from crop residue burns. *J. Agric. Food Chem.* **2003**, *51*, 5047−5051.
(10) Qiu, Y. P.; Xiao, X. Y.; Cheng, H. Y.; Zhou, Z. L.; Sheng, G. D. Influence of environmental factors on pesticide adsorption by black carbon: pH and model dissolved organic matter. *Environ. Sci. Technol.* **2009**, *43*, 4973−4978.
(11) Pignatello, J. J.; Kwon, S.; Lu, Y. F. Effect of natural organic substances on the surface and adsorptive properties of environmental black carbon (char): Attenuation of surface activity by humic and fulvic acids. *Environ. Sci. Technol.* **2006**, *40*, 7757−7763.
(12) Jiang, H.; Adams, C. Treatability of chloro-s-triazines by conventional drinking water treatment technologies. *Water Res.* **2006**, *40*, 1657−1667.
(13) Spokas, K. A.; Koskinen, W. C.; Baker, J. M.; Reicosky, D. C. Impacts of woodchip biochar additions on greenhouse gas production and sorption/degradation of two herbicides in a Minnesota soil. *Chemosphere* **2009**, *77*, 574−581.
(14) Chen, G. C.; Shan, X. Q.; Wang, Y. S.; Pei, Z. G.; Shen, X. E.; Wen, B.; Owens, G. Effects of copper, lead, and cadmium on the sorption and desorption of atrazine onto and from carbon nanotubes. *Environ. Sci. Technol.* **2008**, *42*, 8297−8302.
(15) Schwarzenbach, R. P.; Gschwend, P. M.; Imboden, D. M. *Environmental Organic Chemistry*; Wiley-Interscience: New York, 1993.
(16) Nguyen, T. H.; Cho, H. H.; Poster, D. L.; Ball, W. P. Evidence for a pore-filling mechanism in the adsorption of aromatic hydrocarbons to a natural wood char. *Environ. Sci. Technol.* **2007**, *41*, 1212−1217.
(17) Chan, K. Y.; Van Zwieten, L.; Meszaros, I.; Downie, A.; Joseph, S. Using poultry litter biochars as soil amendments. *Aust. J. Soil Res.* **2008**, *46*, 437−444.
(18) Bannon, D. I.; Drexler, J. W.; Fent, G. M.; Casteel, S. W.; Hunter, P. J.; Brattin, W. J.; Major, M. A. Evaluation of small arms range soils for metal contamination and lead bioavailability. *Environ. Sci. Technol.* **2009**, *43*, 9071−9076.
(19) Mason, Y.; Ammann, A. A.; Ulrich, A.; Sigg, L. Behavior of heavy metals, nutrients, and major components during roof runoff infiltration. *Environ. Sci. Technol.* **1999**, *33*, 1588−1597.
(20) Lima, I. M.; Boateng, A. A.; Klasson, K. T. Pyrolysis of broiler manure: Char and product gas characterization. *Ind. Eng. Chem. Res.* **2009**, *48*, 1292−1297.
(21) Uchimiya, M.; Lima, I. M.; Klasson, K. T.; Chang, S.; Wartelle, L. H.; Rodgers, J. E. Immobilization of heavy metal ions (Cu^{II}, Cd^{II}, Ni^{II}, Pb^{II}) by broiler litter-derived biochars in water and soil. *J. Agric. Food Chem.* **2010**, *58*, 5538−5544.
(22) Cao, X. D.; Ma, L. N.; Gao, B.; Harris, W. Dairy-manure derived biochar effectively sorbs lead and atrazine. *Environ. Sci. Technol.* **2009**, *43*, 3285−3291.
(23) Das, D. D.; Schnitzer, M. I.; Monreal, C. M.; Mayer, P. Chemical composition of acid-base fractions separated from biooil derived by fast pyrolysis of chicken manure. *Bioresour. Technol.* **2009**, *100*, 6524−6532.
(24) Koelmans, A. A.; Jonker, M. T. O.; Cornelissen, G.; Bucheli, T. D.; Van Noort, P. C. M.; Gustafsson, O. Black carbon: The reverse of its dark side. *Chemosphere* **2006**, *63*, 365−377.
(25) Kleineidam, S.; Schuth, C.; Grathwohl, P. Solubility-normalized combined adsorption-partitioning sorption isotherms for organic pollutants. *Environ. Sci. Technol.* **2002**, *36*, 4689−4697.
(26) Zhou, Z. L.; Shi, D. J.; Qiu, Y. P.; Sheng, G. D. Sorptive domains of pine chars as probed by benzene and nitrobenzene. *Environ. Pollut.* **2010**, *158*, 201−206.
(27) Keiluweit, M.; Kleber, M. Molecular-level interactions in soils and sediments: The role of aromatic pi-systems. *Environ. Sci. Technol.* **2009**, *43*, 3421−3429.
(28) Chiou, C. T.; Kile, D. E. Deviations from sorption linearity on soils of polar and nonpolar organic compounds at low relative concentrations. *Environ. Sci. Technol.* **1998**, *32*, 338−343.
(29) Hsu, N. H.; Wang, S. L.; Lin, Y. C.; Sheng, G. D.; Lee, J. F. Reduction of Cr(VI) by crop-residue-derived black carbon. *Environ. Sci. Technol.* **2009**, *43*, 8801−8806.
(30) Polo, M. S.; Utrilla, J. R. Adsorbent-adsorbate interactions in the adsorption of Cd(II) and Hg(II) on ozonized activated carbons. *Environ. Sci. Technol.* **2002**, *36*, 3850−3854.
(31) Wang, Y. S.; Shan, X. Q.; Feng, M. H.; Chen, G. C.; Pei, Z. G.; Wen, B.; Liu, T.; Xie, Y. N.; Owens, G. Effects of copper, lead, and cadmium on the sorption of 2,4,6-trichlorophenol onto and desorption from wheat ash and two commercial humic acids. *Environ. Sci. Technol.* **2009**, *43*, 5726−5731.
(32) Huang, C. H.; Stone, A. T. Transformation of the plant growth regulator daminozide (Alar) and structurally related compounds with Cu-II ions: Oxidation versus hydrolysis. *Environ. Sci. Technol.* **2003**, *37*, 1829−1837.
(33) Sobek, A.; Stamm, N.; Bucheli, T. D. Sorption of phenyl urea herbicides to black carbon. *Environ. Sci. Technol.* **2009**, *43*, 8147−8152.
(34) Ghose, A. K.; Crippen, G. M. Atomic physicochemical parameters for three-dimensional-structure-directed quantitative structure-activity relationships. 2. Modeling dispersive and hydrophobic interactions. *J. Chem. Inf. Comput. Sci.* **1987**, *27*, 21−35.
(35) Uchimiya, M.; Lima, I. M.; Klasson, K. T.; Wartelle, L. H. Contaminant immobilization and nutrient release by biochar soil amendment: Roles of natural organic matter. *Chemosphere* **2010**, *80*, 935−940.

Received for review June 4, 2010. Revised manuscript received October 21, 2010. Accepted October 22, 2010. Mention of trade names or commercial products in this publication is solely for the purpose of providing specific information and does not imply recommendation or endorsement by the U.S. Department of Agriculture.